Complementarity and equivalent formulations via nonlinear programming: numerical results on multi-rigid-body contact problems with Coulomb friction *

Roberto Andreani † Ana Friedlander ‡ Margarida P. Mello §
Sandra A. Santos ¶

September 11, 2002

Abstract

In this work we show that the complementarity problems that model three-dimensional multi-rigid-body contact problems with friction may be formulated as equivalent nonlinear bound-constrained optimization problems. This transformation preserves the smoothness of the original problem, at the price of increasing the number of variables. One may thus take advantage of existing codes for bound-constrained optimization. Preliminary numerical results indicate the approach is promising.

Keywords: complementarity problem; bound-constrained minimization; multi-rigid-body contact problem; Coulomb friction.

Resumo

Neste trabalho mostramos que os problemas de complementaridade que modelam problemas tridimensionais de contato envolvendo múltiplos corpos rígidos com fricção podem ser formulados como problemas equivalentes de otimização em caixas. Esta transformação preserva a suavidade do problema original sob pena de aumentar o número de variáveis. Pode-se assim tirar vantagem dos códigos existentes para otimização em caixas. Resultados numéricos preliminares indicam que esta abordagem é promissora.

Palavras-chave: problema de complementaridade; minimização em caixas; problema de contato com múltiplos corpos rígidos; lei de fricção de Coulomb.

---

*This research has been supported by PRONEX-Optimization, CNPq, FAPESP and Faep-Unicamp.

†Institute of Mathematics, Statistics and Scientific Computation, State University of Campinas, CP 6065, Campinas, SP, 13081-970, Brazil. e-mail: andreani@ime.unicamp.br

‡Institute of Mathematics, Statistics and Scientific Computation, State University of Campinas, CP 6065, Campinas, SP, 13081-970, Brazil. e-mail: friedlan@ime.unicamp.br

§Institute of Mathematics, Statistics and Scientific Computation, State University of Campinas, CP 6065, Campinas, SP, 13081-970, Brazil. e-mail: margarid@ime.unicamp.br

¶Institute of Mathematics, Statistics and Scientific Computation, State University of Campinas, CP 6065, Campinas, SP, 13081-970, Brazil. e-mail: sandra@ime.unicamp.br

1 Introduction

A typical approach to the motion planning problem of several rigid bodies in contact is based on time discretization. This leads to a sequence of problems, one for each time frame. Pang and Trinkle [15, 16, 17] give several formulations for the single time frame problem, in which the accelerations of a set of rigid three-dimensional bodies in contact, in the presence of friction, are computed. This problem may be classified, in its most general version (Coulomb friction law) as a mixed nonlinear complementarity problem (mixed NCP, or MNCP). Relaxations and/or special cases give rise to simpler problems, namely linear complementarity (LCP) ones. A recent thesis work [18] developed a fully-implicit time-stepping scheme for the simulation of the multi-rigid-body contact problem with Coulomb friction. A central feature of the algorithm presented therein is the NCP solver employed at each time step.

The work of [15] carefully develops the theory behind both formulations (MNCP and LCP). Nevertheless, the more algorithmically inclined paper [16], after surveying related work and previous approaches to this problem, tackles only the LCP relaxation in the numerical experiments section. Two algorithms for solving LCP's are compared: the classical Lemke's algorithm and a new interior point method.

In this work we show that, under suitable (but not overly restrictive) assumptions, these complementarity problems may be formulated as equivalent nonlinear bound-constrained optimization problems. This transformation preserves the smoothness of the original problem, at the price of increasing the number of variables. One may thus take advantage of existing codes for bound-constrained optimization.

Numerical experiments are presented, using the software easy, developed by the Optimization Group of the Department of Applied Mathematics at the State University of Campinas, Unicamp, see [8, 12]. We conclude that the approach is promising for solving the model with friction.

2 Complementarity formulations: MNCP and LCP

2.1 The contact model

We will adopt the conventions and notation of [16], which we present summarized in this section. The model assumes the following six hypotheses: (1) the bodies are rigid; (2) the normal direction at each contact is well-defined; (3) dry friction exists at each contact point; (4) each manipulator joint has one degree of freedom; (5) the manipulator has no closed loops formed by the links and joints, closed loops involving (unilateral) contacts are allowed; (6) all links are connected (at least indirectly) to a grounded link.

The problem allows for n_{obj} objects, n_{man} manipulator links, n_θ manipulator joints, and n_c contact points at (the beginning of) the current time period. The contact points are split into two categories: rolling ($n_{\mathcal{R}}$) and sliding ($n_{\mathcal{S}}$), where $n_{\mathcal{R}} + n_{\mathcal{S}} = n_c$. Each contact point j is associated with a unique pair (i, k) of objects in contact and its location defines the origin of the contact frame C_j. This frame comprises three directions: $\hat{\boldsymbol{n}}_j$ (the contact normal points inward with respect to body i, if $i < k$, and outward otherwise), $\hat{\boldsymbol{t}}_j$ and $\hat{\boldsymbol{o}}_j$ (the last two generate the contact tangent plane and satisfy $\hat{\boldsymbol{n}}_j \times \hat{\boldsymbol{t}}_j = \hat{\boldsymbol{o}}_j$). The contact force acting on body i through contact j and expressed in C_j is given by

$\boldsymbol{c}_{i,j} = ((c_{i,j})_n, (c_{i,j})_t, (c_{i,j})_o)^T$. Notice that Newton's third law implies $\boldsymbol{c}_{i,j} = -\boldsymbol{c}_{k,j}$. Let $\boldsymbol{W}_{i,j}$ be the 6×3 wrench matrix that transforms contact forces $\boldsymbol{c}_{i,j}$ into equivalent wrench (generalized force) in the body frame B_i.

Letting $\boldsymbol{M}_{\text{obj},i}$ denote the 6×6 positive definite and symmetric mass matrix of object i, $\boldsymbol{g}_{\text{obj},i}$ denote the external generalized force 6-vector acting on object i, $\boldsymbol{h}_{\text{obj},i}$ denote the 6-vector of velocity product terms and $\ddot{\boldsymbol{q}}_i$ denote the generalized 6-vector acceleration of object i, the Newton-Euler equation governing the motion of object i is

$$\sum_{j \in \mathcal{B}_i} \boldsymbol{W}_{i,j} \boldsymbol{c}_{i,j} + \boldsymbol{g}_{\text{obj},i} + \boldsymbol{h}_{\text{obj},i} = \boldsymbol{M}_{\text{obj},i} \ddot{\boldsymbol{q}}_i, \tag{1}$$

where $\mathcal{B}_i$ is the index set of contact points that involve body i. Recasting (1) in matrix form we obtain

$$\boldsymbol{W}\boldsymbol{c} + \boldsymbol{g}_{\text{obj}} + \boldsymbol{h}_{\text{obj}} = \boldsymbol{M}_{\text{obj}} \ddot{\boldsymbol{q}}. \tag{2}$$

A similar development produces the dynamic equations of the manipulator:

$$\boldsymbol{\tau} - (\boldsymbol{J}^T \boldsymbol{c} + \boldsymbol{g}_{\text{man}} + \boldsymbol{h}_{\text{man}}) = \boldsymbol{M}_{\text{man}} \ddot{\boldsymbol{\theta}}, \tag{3}$$

where $\boldsymbol{\tau}$ is the n_θ vector of joint efforts, $\boldsymbol{J}$ is the $3n_c \times n_\theta$ global Jacobian matrix, $\boldsymbol{M}_{\text{man}}$ is the $n_\theta \times n_\theta$ positive definite and symmetric inertia matrix, $\boldsymbol{g}_{\text{man}}$ and $\boldsymbol{h}_{\text{man}}$ are the n_θ vectors of joint efforts induced by external wrenches and velocity product wrenches, respectively, and $\ddot{\boldsymbol{\theta}}$ is the n_θ vector of joint accelerations.

Equations (2) and (3) may be rewritten by grouping together the normal, tangential and orthonormal components of vectors and matrices involved, as follows:

$$\begin{aligned} \boldsymbol{W}_n \boldsymbol{c}_n + \boldsymbol{W}_t \boldsymbol{c}_t + \boldsymbol{W}_o \boldsymbol{c}_o + \boldsymbol{g}_{\text{obj}} + \boldsymbol{h}_{\text{obj}} &= \boldsymbol{M}_{\text{obj}} \ddot{\boldsymbol{q}} & (4) \\ \boldsymbol{\tau} - (\boldsymbol{J}_n^T \boldsymbol{c}_n + \boldsymbol{J}_t^T \boldsymbol{c}_t + \boldsymbol{J}_o^T \boldsymbol{c}_o + \boldsymbol{g}_{\text{man}} + \boldsymbol{h}_{\text{man}}) &= \boldsymbol{M}_{\text{man}} \ddot{\boldsymbol{\theta}}. & (5) \end{aligned}$$

It is worth mentioning that $\boldsymbol{W}_n$, $\boldsymbol{W}_t$ and $\boldsymbol{W}_o$ are $6n_{\text{obj}} \times n_c$ matrices, whereas $\boldsymbol{J}_n$, $\boldsymbol{J}_t$ and $\boldsymbol{J}_o$ have dimension $n_c \times n_\theta$.

Let $\boldsymbol{v}_j = (v_{jn}, v_{jt}, v_{jo})^T$ and $\boldsymbol{a}_j = (a_{jn}, a_{jt}, a_{jo})^T$, for $j = 1, \ldots, n_c$, be the relative linear velocity and acceleration vectors, expressed in frame C_j. Grouping together the normal, tangential and orthonormal components of these vectors, for each subset we have:

$$\begin{aligned} \boldsymbol{v}_\alpha &= \boldsymbol{W}_\alpha^T \dot{\boldsymbol{q}} - \boldsymbol{J}_\alpha \dot{\boldsymbol{\theta}}, & \alpha \in \{n, t, o\}, \quad (6) \\ \boldsymbol{a}_\alpha &= \boldsymbol{W}_\alpha^T \ddot{\boldsymbol{q}} - \boldsymbol{J}_\alpha \ddot{\boldsymbol{\theta}} + \dot{\boldsymbol{W}}_\alpha^T \dot{\boldsymbol{q}} - \dot{\boldsymbol{J}}_\alpha \dot{\boldsymbol{\theta}}, & \alpha \in \{n, t, o\}. \quad (7) \end{aligned}$$

The normal component $\boldsymbol{v}_n$ is always zero, but the tangent plane contribution $v_{jt}^2 + v_{jo}^2$ at a sliding contact is nonzero, whereas it is zero at a rolling contact. Thus $\boldsymbol{v}$, the velocity at the beginning of the current time frame, calculated in (6), must satisfy these conditions. The normal component of relative acceleration must be nonnegative to prevent interpenetration at the contact points. Therefore the unknown $\boldsymbol{a}_n$ must satisfy

$$\boldsymbol{a}_n \geq 0, \tag{8}$$

and if it turns out to be zero (resp., positive), this means the contact will be maintained (resp., broken).

The components of $\boldsymbol{c}$ must satisfy Coulomb's law, i.e., they must belong to the friction cone defined by

$$c_{jt}^2 + c_{jo}^2 \leq \mu_j^2 c_{jn}^2, \quad \text{for } j = 1, \ldots, n_c, \tag{9}$$

where μ_j is the friction coefficient at the j-th contact point. Furthermore, the contact forces are compressive:

$$c_{jn} \geq 0, \quad \text{for } j = 1, \ldots, n_c. \tag{10}$$

For each sliding contact, the force vector must lie on the boundary of the friction cone, with its friction component in the opposite direction of the relative sliding velocity, which is equivalent to (11) below. Similar equations (12) must hold at the rolling contacts. Note that these equations are redundant unless $a_{jt}^2 + a_{jo}^2 \neq 0$, which is the case if the rolling contact is to become a sliding contact.

$$\mu_j \, c_{jn} \, v_{j\alpha} + c_{j\alpha} \sqrt{v_{jt}^2 + v_{jo}^2} = 0, \quad \text{for } \alpha \in \{t, o\} \text{ and } j \in \mathcal{S} \tag{11}$$

$$\mu_j \, c_{jn} \, a_{j\alpha} + c_{j\alpha} \sqrt{a_{jt}^2 + a_{jo}^2} = 0, \quad \text{for } \alpha \in \{t, o\} \text{ and } j \in \mathcal{R}. \tag{12}$$

The *three-dimensional multi-rigid-body contact problem with Coulomb friction law* may be stated as: given $\boldsymbol{q}$, $\dot{\boldsymbol{q}}$, $\boldsymbol{g}_{\text{obj}}$, $\boldsymbol{h}_{\text{obj}}$, $\boldsymbol{M}_{\text{obj}}$, $\boldsymbol{\theta}$, $\dot{\boldsymbol{\theta}}$, $\boldsymbol{\tau}$, $\boldsymbol{g}_{\text{man}}$, $\boldsymbol{h}_{\text{man}}$, $\boldsymbol{M}_{\text{man}}$ and the $\boldsymbol{W}$ and $\boldsymbol{J}$ matrices, determine $\ddot{\boldsymbol{q}}$, $\ddot{\boldsymbol{\theta}}$, $\boldsymbol{c}_n$, $\boldsymbol{c}_t$, $\boldsymbol{c}_o$, $\boldsymbol{a}_n$, $\boldsymbol{a}_t$, $\boldsymbol{a}_o$, satisfying equations (4), (5), (7)–(12), and the complementarity condition

$$\boldsymbol{c}_n^T \boldsymbol{a}_n = 0. \tag{13}$$

The above formulation of the three-dimensional contact problem involves linear constraints (4), (5), (7), (8), (10), (11); complementarity (13) and nonlinear ones (9), (12). Constraints (9) are encompassed by (11) for the sliding contacts, since, in this case, vector $\boldsymbol{c}$ must belong to the boundary of the friction cone. Thus in fact, nonlinearity is restricted to the members of (9) corresponding to the rolling contacts and (12). If the concrete instance to be solved does not present rolling contacts, the contact problem may be transformed into an equivalent LCP. If it does contain rolling contacts, one may cast it as an MNCP, but not as an LCP. It is, nevertheless, possible to replace (9) corresponding to the rolling contacts and (12) with an approximate model, the so-called *friction pyramid law*, [15]:

$$\begin{aligned} \max\{|c_{jt}|, |c_{jo}|\} &\leq \mu_j c_{jn}, && \text{for all } j \in \mathcal{R} && (14) \\ \mu_j \; c_{jn} \; |a_{j\alpha}| + a_{j\alpha} \; c_{j\alpha} &= 0, && \text{for } \alpha \in \{t, o\} \text{ and } j \in \mathcal{R}. && (15) \end{aligned}$$

Therefore, the *three-dimensional multi-rigid-body contact problem with friction pyramid law*[1] is obtained from the previous problem by replacing (9) corresponding to the rolling contacts and (12) with (14)–(15). Figure 1 depicts the Coulomb cone together with the pyramid, its polyhedral approximation.

[1] The name of the problem is somewhat misleading, since the Coulomb law still holds at the sliding contacts.

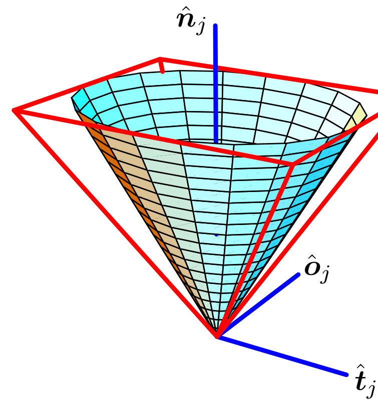

Figure 1: Coulomb cone and pyramid

2.2 Casting the model as an MNCP/LCP

Although the formats of the linear complementarity problem (LCP) and the nonlinear complementarity problem (NCP) are standard in the literature, this is not the case for the mixed nonlinear complementarity problem (MNCP). In this work the following format, see [14], is adopted:

$$\text{(MNCP)} \qquad \begin{array}{l} \text{Given } \boldsymbol{f} : \mathbb{R}^{n+m} \to \mathbb{R}^n \text{ and } \boldsymbol{g} : \mathbb{R}^{n+m} \to \mathbb{R}^p \\ \text{find } \boldsymbol{u} \in \mathbb{R}^n \text{ and } \boldsymbol{v} \in \mathbb{R}^m \text{ such that} \\ \boldsymbol{u} \geq 0,\ \ \boldsymbol{f}(\boldsymbol{u}, \boldsymbol{v}) \geq 0,\ \ \boldsymbol{u}^T \boldsymbol{f}(\boldsymbol{u}, \boldsymbol{v}) = 0 \\ \boldsymbol{g}(\boldsymbol{u}, \boldsymbol{v}) = 0. \end{array}$$

In the LCP, $m = 0$, there is no function $\boldsymbol{g}$ and $\boldsymbol{f}$ is affine, e.g., $\boldsymbol{f}(\boldsymbol{u}) = \boldsymbol{Q}\boldsymbol{u} + \boldsymbol{d}$.

In order to arrive at either format, some amount of preprocessing is necessary. To obtain the MNCP we must go through the following steps: (i) Equations (4) and (5) are premultiplied by the appropriate inverses ($\boldsymbol{M}_{\mathrm{obj}}$ and $\boldsymbol{M}_{\mathrm{man}}$ are assumed to be positive definite) so the vectors $\ddot{\boldsymbol{q}}$ and $\ddot{\boldsymbol{\theta}}$ may be expressed as an affine function of the remaining unknowns and thus eliminated from the problem. (ii) All variables are arranged in two groups, corresponding to the sliding and rolling contacts, respectively, and then equation (11) is used to eliminate $\boldsymbol{c}_{\mathcal{S}t}$ and $\boldsymbol{c}_{\mathcal{S}o}$, so that only $\boldsymbol{c}_{\mathcal{S}n}$ remains after the substitution. (iii) The problem is further simplified by noting that a subset of equations lead to closed formulas for $\boldsymbol{a}_{\mathcal{S}t}$ and $\boldsymbol{a}_{\mathcal{S}o}$ as functions of the contact forces. These equations may be left out of the formulation and used to compute $\boldsymbol{a}_{\mathcal{S}t}$ and $\boldsymbol{a}_{\mathcal{S}o}$ after the problem is solved. (iv) Finally, equations (9) (only defined for rolling contacts) and (12) are replaced by the equivalent set of constraints:

$$\begin{array}{rcll} \mu_j^2 c_{jn}^2 - c_{jt}^2 - c_{jo}^2 & = & s_j, & \text{for } j \in \mathcal{R} \\ \mu_j c_{jn} a_{j\alpha} + c_{j\alpha}\lambda_j & = & 0, & \text{for } \alpha \in \{t, o\} \text{ and } j \in \mathcal{R} \\ \lambda_j\, s_j & = & 0, & \text{for } j \in \mathcal{R} \\ \lambda_j,\, s_j & \geq & 0, & \text{for } j \in \mathcal{R}. \end{array}$$

Letting $\boldsymbol{u} = (\boldsymbol{c}_{\mathcal{S}n}^T, \boldsymbol{c}_{\mathcal{R}n}^T, \boldsymbol{\lambda}_{\mathcal{R}}^T)^T$, $\boldsymbol{v} = (\boldsymbol{c}_{\mathcal{R}t}^T, \boldsymbol{c}_{\mathcal{R}o}^T, \boldsymbol{a}_{\mathcal{R}t}^T, \boldsymbol{a}_{\mathcal{R}o}^T)^T$, $\boldsymbol{f}(\boldsymbol{u}, \boldsymbol{v}) = (\boldsymbol{a}_{\mathcal{S}n}^T, \boldsymbol{a}_{\mathcal{R}n}^T, \boldsymbol{s}_{\mathcal{R}}^T)^T$, where

$$\begin{pmatrix} \boldsymbol{a}_{\mathcal{S}n} \\ \boldsymbol{a}_{\mathcal{R}n} \end{pmatrix} = \tilde{\boldsymbol{A}}_1 \begin{pmatrix} \boldsymbol{c}_{\mathcal{S}n} \\ \boldsymbol{c}_{\mathcal{R}n} \\ \boldsymbol{c}_{\mathcal{R}t} \\ \boldsymbol{c}_{\mathcal{R}o} \end{pmatrix} + \begin{pmatrix} \boldsymbol{b}_{\mathcal{S}n} \\ \boldsymbol{b}_{\mathcal{R}n} \end{pmatrix} \tag{16}$$

$$s_j = \mu_j^2 c_{jn}^2 - c_{jt}^2 - c_{jo}^2, \quad \text{for } j \in \mathcal{R} \tag{17}$$

and $\boldsymbol{g}(\boldsymbol{u}, \boldsymbol{v}) = 0$ is given by

$$\mu_j c_{jn} a_{j\alpha} + c_{j\alpha}\lambda_j = 0, \quad \text{for } \alpha \in \{t, o\} \text{ and } j \in \mathcal{R} \tag{18}$$

$$\begin{pmatrix} \boldsymbol{a}_{\mathcal{R}t} \\ \boldsymbol{a}_{\mathcal{R}o} \end{pmatrix} - \left(\tilde{\boldsymbol{A}}_2 \begin{pmatrix} \boldsymbol{c}_{\mathcal{S}n} \\ \boldsymbol{c}_{\mathcal{R}n} \\ \boldsymbol{c}_{\mathcal{R}t} \\ \boldsymbol{c}_{\mathcal{R}o} \end{pmatrix} + \begin{pmatrix} \boldsymbol{b}_{\mathcal{R}t} \\ \boldsymbol{b}_{\mathcal{R}o} \end{pmatrix} \right) = 0, \tag{19}$$

so the dimensions n, m and p are respectively given by $n_{\mathcal{S}} + 2n_{\mathcal{R}}$, $4n_{\mathcal{R}}$ and $4n_{\mathcal{R}}$. Matrix $\tilde{\boldsymbol{A}} = (\tilde{\boldsymbol{A}}_1{}^T, \tilde{\boldsymbol{A}}_2{}^T)^T$ and vector $\boldsymbol{b} = (\boldsymbol{b}_{\mathcal{S}n}^T, \boldsymbol{b}_{\mathcal{R}n}^T, \boldsymbol{b}_{\mathcal{R}t}^T, \boldsymbol{b}_{\mathcal{R}o}^T)^T$ depend on $\boldsymbol{W}$, $\boldsymbol{M}_{\mathrm{obj}}$, $\boldsymbol{M}_{\mathrm{man}}$, $\boldsymbol{g}_{\mathrm{obj}}$, $\boldsymbol{h}_{\mathrm{obj}}$, $\boldsymbol{g}_{\mathrm{man}}$, $\boldsymbol{h}_{\mathrm{man}}$, $\boldsymbol{\tau}$, $\dot{\boldsymbol{W}}$,$\dot{\boldsymbol{J}}$,$\dot{\boldsymbol{q}}$, $\dot{\boldsymbol{\theta}}$, see [16] for complete expressions. It should be noted, however, that the MNCP formulation in [16] slightly differs from the one given here in the sense that we do allow free variables, whereas in [16] the free variables are split into two nonnegative parts.

The deduction of the LCP is similar. Steps (i) through (iii) are the same. The new step (iv) consists of: (iv-a) splitting $\boldsymbol{a}_{\mathcal{R}\alpha} = \boldsymbol{a}_{\mathcal{R}\alpha}^+ - \boldsymbol{a}_{\mathcal{R}\alpha}^-$, with $\boldsymbol{a}_{\mathcal{R}\alpha}^+$, $\boldsymbol{a}_{\mathcal{R}\alpha}^-$ nonnegative, for $\alpha \in \{t, o\}$ (see Lemma 1 of [15, p. 207]); (iv-b) introducing the nonnegative slack variables

$$s_{j\alpha}^+ = \mu_j c_{jn} + c_{j\alpha}, \qquad s_{j\alpha}^- = \mu_j c_{jn} - c_{j\alpha}, \quad \text{for } \alpha \in \{t, o\} \text{ and } j \in \mathcal{R}.$$

These slack variables must satisfy complementarity conditions with the corresponding tangential contact accelerations. (iv-c) The vectors $\boldsymbol{c}_{\mathcal{R}t}$ and $\boldsymbol{c}_{\mathcal{R}o}$ are expressed as functions of the slack variables and thus eliminated. The elements of the LCP formulation are:

$$\begin{aligned} \boldsymbol{u} &= (\boldsymbol{c}_{\mathcal{S}n}^T, \boldsymbol{c}_{\mathcal{R}n}^T, (\boldsymbol{s}_{\mathcal{R}t}^+)^T, (\boldsymbol{s}_{\mathcal{R}o}^+)^T, (\boldsymbol{a}_{\mathcal{R}t}^-)^T, (\boldsymbol{a}_{\mathcal{R}o}^-)^T)^T \\ \text{and} \qquad \boldsymbol{f}(\boldsymbol{u}) &= (\boldsymbol{a}_{\mathcal{S}n}^T, \boldsymbol{a}_{\mathcal{R}n}^T, (\boldsymbol{a}_{\mathcal{R}t}^+)^T, (\boldsymbol{a}_{\mathcal{R}o}^+)^T, (\boldsymbol{s}_{\mathcal{R}t}^-)^T, (\boldsymbol{s}_{\mathcal{R}o}^-)^T)^T. \end{aligned} \tag{20}$$

Formulas for the $(n_{\mathcal{S}} + 5n_{\mathcal{R}}) \times (n_{\mathcal{S}} + 5n_{\mathcal{R}})$ matrix $\boldsymbol{Q}$ and vector $\boldsymbol{d}$ are given in [16], denoted therein by $\boldsymbol{M}$ and $\boldsymbol{r}$, respectively.

3 Equivalent formulations

Methods for solving complementarity problems may be classified in two groups: those that involve algorithms specially developed for this kind of problems ([5, 10, 11]) and those that work on the minimization of a merit function created to represent the problem, in the sense that it will be zero only at the solutions of the complementarity problem ([1, 9, 10, 11, 14]). This work adopts the second approach. Ferris and Pang [6] provide a more detailed classification, with the respective references.

The MNCP is replaced with the following optimization problem:

$$
\begin{array}{llll}
\text{(MNCPOpt)} & \min & \frac{1}{2}\left(\|\boldsymbol{f}(\boldsymbol{u},\boldsymbol{v})-\boldsymbol{z}\|_2^2+\|\boldsymbol{g}(\boldsymbol{u},\boldsymbol{v})\|_2^2+(\boldsymbol{u}^T\boldsymbol{z})^2\right) \\
& \text{s.t.} & \boldsymbol{u},\boldsymbol{z} \ \geq \ 0.
\end{array}
$$

Theorem 3 below states that under suitable conditions, stationary points are also global solutions of (MNCPOpt). Furthermore this problem is as smooth as the original MNCP. The advantadge of this approach is that it opens the possibility of applying any available nonlinear optimization code to solve the MNCP, no need to program a specialized algorithm. On the other hand, this formulation involves the additional vector $\boldsymbol{z}$, which increases the dimension of the problem. Nevertheless, the computational tests performed so far show promise for this kind of approach, as can be seen in the numerical experiments section.

Theorem 1 *If* $(\boldsymbol{u}^*,\boldsymbol{v}^*,\boldsymbol{z}^*)$ *is a stationary point of* (MNCPOpt) *and the Schur complement of* $\boldsymbol{g}_{\boldsymbol{v}}(\boldsymbol{u}^*,\boldsymbol{v}^*)$ *in the Jacobian*

$$\boldsymbol{J}(\boldsymbol{u}^*,\boldsymbol{v}^*)=\left[\begin{array}{cc} \boldsymbol{f}_{\boldsymbol{u}}(\boldsymbol{u}^*,\boldsymbol{v}^*) & \boldsymbol{f}_{\boldsymbol{v}}(\boldsymbol{u}^*,\boldsymbol{v}^*) \\ \boldsymbol{g}_{\boldsymbol{u}}(\boldsymbol{u}^*,\boldsymbol{v}^*) & \boldsymbol{g}_{\boldsymbol{v}}(\boldsymbol{u}^*,\boldsymbol{v}^*) \end{array}\right]$$

is a row sufficient[2] *S-matrix*[3]*, then* $(\boldsymbol{u}^*,\boldsymbol{v}^*)$ *is a solution of* (MNCP).

Proof Let $\boldsymbol{\mu}^*$ and $\boldsymbol{\gamma}^*$ be the Lagrange multipliers associated with $\boldsymbol{u}\geq 0$ and $\boldsymbol{z}\geq 0$, respectively, at the stationaty point $(\boldsymbol{u}^*,\boldsymbol{v}^*,\boldsymbol{z}^*)$. In order to simplify notation, we also let

$$
\begin{array}{lrcl}
& \boldsymbol{w}^* & = & \boldsymbol{f}_u^T(\boldsymbol{u}^*,\boldsymbol{v}^*)-\boldsymbol{z}^* \\
\text{and} & \theta^* & = & \boldsymbol{u}^{*T}\boldsymbol{z}^*.
\end{array}
$$

Using the above definitions, the equations satisfied by the stationary point $(\boldsymbol{u}^*,\boldsymbol{v}^*,\boldsymbol{z}^*)$ are

$$\boldsymbol{f}_{\boldsymbol{u}}^T(\boldsymbol{u}^*,\boldsymbol{v}^*)\boldsymbol{w}^*+\boldsymbol{g}_{\boldsymbol{u}}^T(\boldsymbol{u}^*,\boldsymbol{v}^*)\boldsymbol{g}(\boldsymbol{u}^*,\boldsymbol{v}^*)+\theta^*\boldsymbol{z}^*-\boldsymbol{\mu}^* = 0 \tag{21}$$

$$\boldsymbol{f}_{\boldsymbol{v}}^T(\boldsymbol{u}^*,\boldsymbol{v}^*)\boldsymbol{w}^*+\boldsymbol{g}_{\boldsymbol{v}}^T(\boldsymbol{u}^*,\boldsymbol{v}^*)\boldsymbol{g}(\boldsymbol{u}^*,\boldsymbol{v}^*) = 0 \tag{22}$$

$$-\boldsymbol{w}^*+\theta^*\boldsymbol{u}^*-\boldsymbol{\gamma}^* = 0 \tag{23}$$

$$\boldsymbol{u}^{*T}\boldsymbol{\mu}^* = \boldsymbol{z}^{*T}\boldsymbol{\gamma}^* = 0 \tag{24}$$

$$\boldsymbol{u}^*,\ \boldsymbol{z}^*,\ \boldsymbol{\gamma}^*,\ \boldsymbol{\mu}^* \geq 0. \tag{25}$$

Equation (22) together with the existence of the Schur complement of $\boldsymbol{g}_{\boldsymbol{v}}(\boldsymbol{u}^*,\boldsymbol{v}^*)$ in $\boldsymbol{J}(\boldsymbol{u}^*,\boldsymbol{v}^*)$ imply the following expression for $\boldsymbol{g}(\boldsymbol{u}^*,\boldsymbol{v}^*)$

$$\boldsymbol{g}(\boldsymbol{u}^*,\boldsymbol{v}^*)=-\boldsymbol{g}_{\boldsymbol{v}}^{-T}(\boldsymbol{u}^*,\boldsymbol{v}^*)\left(\boldsymbol{f}_{\boldsymbol{v}}^T(\boldsymbol{u}^*,\boldsymbol{v}^*)\boldsymbol{w}^*\right). \tag{26}$$

[2] A square matrix is *row sufficient* if its transpose is column sufficient. An $n\times n$ matrix $\boldsymbol{A}$ is *column sufficient* if $x_i\,[\boldsymbol{A}\boldsymbol{x}]_i\leq 0$, for $1\leq i\leq n$, implies $x_i\,[\boldsymbol{A}\boldsymbol{x}]_i=0$, for $1\leq i\leq n$.

[3] An $n\times n$ matrix $\boldsymbol{A}$ is an *S-matrix* if there exists $\boldsymbol{x}\geq 0$ such that $\boldsymbol{A}\boldsymbol{x}>0$.

Substituting this expression in (21) we obtain

$$\begin{aligned}
\boldsymbol{f}_{\boldsymbol{u}}^T(\boldsymbol{u}^*,\boldsymbol{v}^*)\boldsymbol{w}^* - \boldsymbol{g}_{\boldsymbol{u}}^T(\boldsymbol{u}^*,\boldsymbol{v}^*)\boldsymbol{g}_{\boldsymbol{v}}^{-T}(\boldsymbol{u}^*,\boldsymbol{v}^*)\boldsymbol{f}_{\boldsymbol{v}}^T(\boldsymbol{u}^*,\boldsymbol{v}^*)\boldsymbol{w}^* + \theta^*\boldsymbol{z}^* - \boldsymbol{\mu}^* &= \\
\Big(\boldsymbol{f}_{\boldsymbol{u}}^T(\boldsymbol{u}^*,\boldsymbol{v}^*) - \boldsymbol{g}_{\boldsymbol{u}}^T(\boldsymbol{u}^*,\boldsymbol{v}^*)\boldsymbol{g}_{\boldsymbol{v}}^{-T}(\boldsymbol{u}^*,\boldsymbol{v}^*)\boldsymbol{f}_{\boldsymbol{v}}^T(\boldsymbol{u}^*,\boldsymbol{v}^*)\Big)\boldsymbol{w}^* + \theta^*\boldsymbol{z}^* - \boldsymbol{\mu}^* &= 0
\end{aligned} \tag{27}$$

Premultiplying each equation in (27) by w_i and taking (23) and (24) into account, it follows, for all i, that

$$w_i^*\left[\left(\boldsymbol{J}(\boldsymbol{u}^*,\boldsymbol{v}^*)/\boldsymbol{g}_{\boldsymbol{v}}(\boldsymbol{u}^*,\boldsymbol{v}^*)\right)^T\boldsymbol{w}^*\right]_i + \theta^{*2}z_i^*u_i^* + \mu_i^*\gamma_i^* = 0. \tag{28}$$

Equation (28) and (25) imply that

$$w_i^*\left[\left(\boldsymbol{J}(\boldsymbol{u}^*,\boldsymbol{v}^*)/\boldsymbol{g}_{\boldsymbol{v}}(\boldsymbol{u}^*,\boldsymbol{v}^*)\right)^T\boldsymbol{w}^*\right]_i \leq 0, \tag{29}$$

for all i. Using the fact that $(\boldsymbol{J}(\boldsymbol{u}^*,\boldsymbol{v}^*)/\boldsymbol{g}_{\boldsymbol{v}}(\boldsymbol{u}^*,\boldsymbol{v}^*))$ is row sufficient, we conclude from (29) that

$$w_i^*\left[\left(\boldsymbol{J}(\boldsymbol{u}^*,\boldsymbol{v}^*)/\boldsymbol{g}_{\boldsymbol{v}}(\boldsymbol{u}^*,\boldsymbol{v}^*)\right)^T\boldsymbol{w}^*\right]_i = 0, \tag{30}$$

for all i. Substituting (30) in (28) and recalling (25), we have that

$$z_i^*u_i^* = 0, \quad \forall i \qquad \Rightarrow \qquad \theta^* = 0 \tag{31}$$

Equations (23), (25), (27) and (31) imply that

$$\boldsymbol{w}^* \leq 0 \quad \text{and} \quad \left(\boldsymbol{J}(\boldsymbol{u}^*,\boldsymbol{v}^*)/\boldsymbol{g}_{\boldsymbol{v}}(\boldsymbol{u}^*,\boldsymbol{v}^*)\right)^T\boldsymbol{w}^* \geq 0.$$

The above conditions and the fact that $(\boldsymbol{J}(\boldsymbol{u}^*,\boldsymbol{v}^*)/\boldsymbol{g}_{\boldsymbol{v}}(\boldsymbol{u}^*,\boldsymbol{v}^*))$ is an S-matrix guarantee that, see [7, Theorem 2.4]

$$\boldsymbol{w}^* = 0. \tag{32}$$

Substituting (32) in (26) we have

$$\boldsymbol{g}(\boldsymbol{u}^*,\boldsymbol{v}^*) = 0. \tag{33}$$

Equations (25), (31), (32) and (33) imply that the feasible solution $(\boldsymbol{u}^*,\boldsymbol{v}^*,\boldsymbol{z}^*)$ has objective value zero. Therefore $(\boldsymbol{u}^*,\boldsymbol{v}^*)$ is a solution of (MNCP). ■

The formulation for the LCP-equivalent optimization problem is easily obtained from (MNCPOpt), using the relationship previously pointed out between the MNCP and the LCP.

$$\text{(LCPOpt)} \qquad \begin{array}{ll} \min & \frac{1}{2}\left(\|\boldsymbol{Q}\boldsymbol{u}+\boldsymbol{d}-\boldsymbol{z}\|_2^2 + (\boldsymbol{u}^T\boldsymbol{z})^2\right) \\ \text{s.t.} & \boldsymbol{u},\boldsymbol{z} \ \geq \ 0. \end{array}$$

The weakest sufficient conditions that assure stationary points of (LCPOpt) to be solutions of (LCP), proved in [2], are that the (LCP) is *feasible*, i.e., there exist $\boldsymbol{u},\boldsymbol{z} \geq 0$ such that $\boldsymbol{Q}\boldsymbol{u}+\boldsymbol{d}-\boldsymbol{z} = 0$, and $\boldsymbol{Q}$ is a row sufficient matrix.

In the context of the three-dimensional multi-rigid-body contact problem with friction, the dimension of the problems are as follows: the number of variables of (MNCPOpt) is

$$\text{size}(\boldsymbol{u}) + \text{size}(\boldsymbol{v}) + \text{size}(\boldsymbol{z}) = (n_{\mathcal{S}} + 2n_{\mathcal{R}}) + 4n_{\mathcal{R}} + (n_{\mathcal{S}} + 2n_{\mathcal{R}}) = 2n_{\mathcal{S}} + 8n_{\mathcal{R}}$$

and the number of variables of (LCPOpt) is

$$\text{size}(\boldsymbol{u}) + \text{size}(\boldsymbol{z}) = (n_{\mathcal{S}} + 5n_{\mathcal{R}}) + (n_{\mathcal{S}} + 5n_{\mathcal{R}}) = 2n_{\mathcal{S}} + 10n_{\mathcal{R}}.$$

4 Numerical experiments

The optimization problems were solved with the code `easy`, developed by the Optimization Group at the State University of Campinas, available at `http://www.ime.unicamp.br/~martinez`. It is a double-precision Fortran 77 implementation of a trust-region Augmented Lagrangian method for large-scale nonlinear programs. See [8, 12] for details.

Simple instances with two SCARA[4] robots grasping a cubic object were generated. The parameters necessary to describe the initial configurations were defined as in [13, p. 240], namely the location of the coordinate systems with origin at the center of mass of the object (O), at the basis of the k-robot (S_k), and at the j-contact frame (C_j), with respect to the fixed palm frame (P). The distance between the origins of P and O are denoted by a. The distance between the origins of P and S_k is b_k. The symmetry of the generated instances implied $b_k \equiv b$. Figure 2 depicts a complete scheme of the rigid system body&robots with the various coordinate systems. The object was a cube with side length $2r$ and the contact points cp_1 and cp_2 were respectively located at the center of opposing vertical faces, see Figure 2. The specific choices for the various parameters were the following: $r = 0.2$ m; $a = 0.5$ m; $b = 0.8$ m; mass of the object $m_{\text{obj}} = 3$ kg; lengths of the links $\ell_1 = 0.4$ m; $\ell_2 = 0.25$ m; $\ell_3 = 0$ m; initial configuration in the Denavit-Hartenberg notation[5]: $\Theta^1 = (\theta_1, \theta_2, -\pi/6, 0)$, $\Theta^2 = (\theta_1 + \pi, \theta_2, -\pi/6, 0)$, with $\theta_1 = \arcsin(\ell_2/(2\ell_1))$, $\theta_2 = -\theta_1 - \pi/6$. The relative velocities between the fingers and the object were set as $v_i = (0, 1, 0)^T, i = 1, 2$. The friction coefficients were $\mu_1 = 0.1$ and $\mu_2 = 0.2$.

4.1 All sliding case

The first tested instance was created with the assumption that both contact points are of the sliding type, so the problem given by (16)-(19) becomes an LCP with four variables. Tentative experiments adopting the equivalent bound-constrained optimization approach were performed in [3]. Using the notation of problem (LCPOpt), the matrix $Q \in \mathbb{R}^{2\times 2}$ was computed in MATLAB, with the aid of the Robotics TOOLBOX [4] and the vector $d \in \mathbb{R}^2$ was randomly generated in $[-5, 5] \times [-5, 5]$. Two hundred tests were *successfully solved*, that is, the objective function value was smaller than 10^{-10} and the chosen tolerance of 10^{-5} for the norm of the projected gradient was achieved in all tests. The final objective

[4]Selective Compliant Articulated Robot for Assembly

[5]The D-H convention assumes different orientations for the various coordinate systems involved, as explained in the Robotics TOOLBOX [4], for instance. These conventions were adopted in the programming of the numerical experiments.

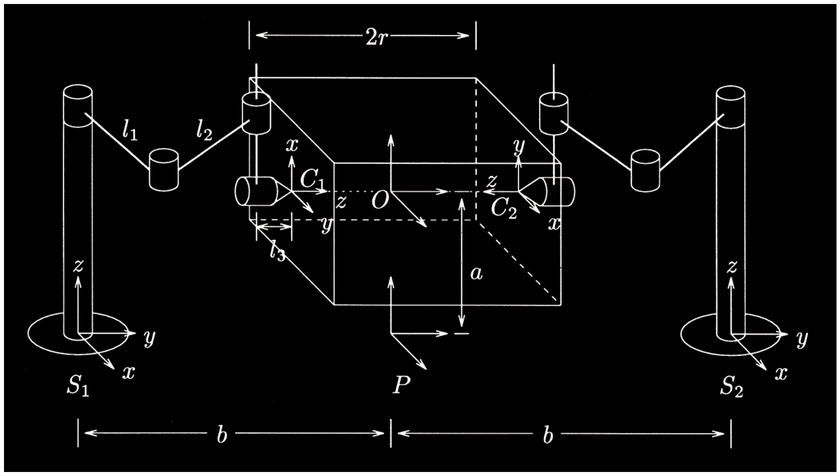

Figure 2: Two-fingered grasp using Scara robots (from [13, p.241])

function values lay in the interval $[10^{-31}, 10^{-10}]$. As far as the complementarity gap is concerned, 43 tests ended with $u^T(Qu + d) = 0$ and for the remaining 157 tests, $10^{-15} \leq |u^T(Qu + d)| \leq 10^{-4}$. In Figure 3, a bar chart of $\lfloor -\log_{10}|u^T(Qu + d)| \rfloor$ *versus* number of tests illustrates the distribution of the absolute value of the gap for the 157 tests that did not reached final value zero.

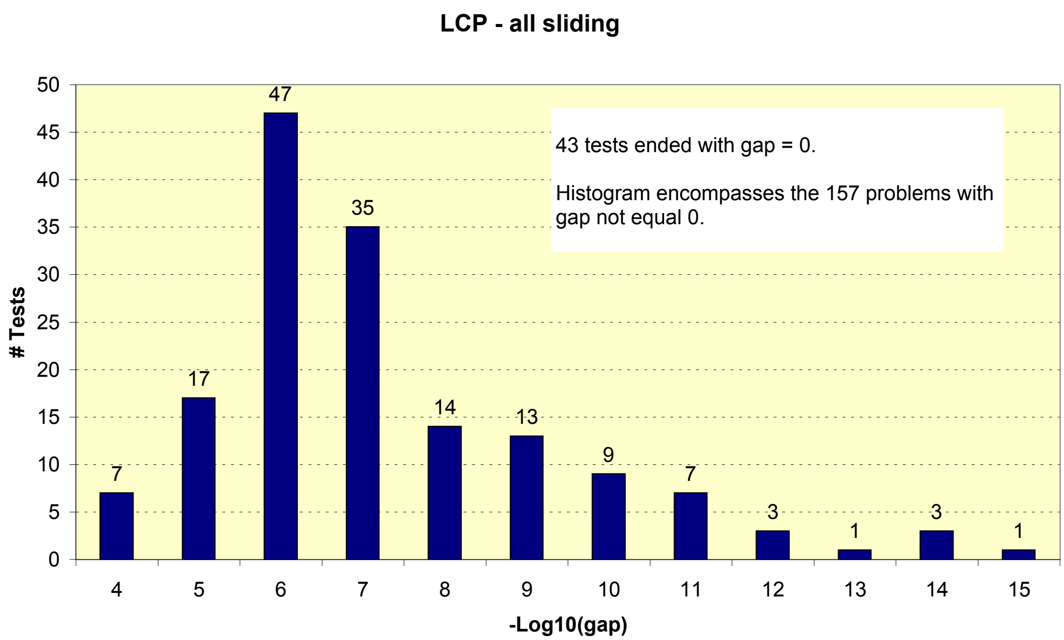

Figure 3: Complementarity gap distribution for all sliding case

4.2 All rolling case

Assuming next that both contacts are rolling, two instances were generated for each problem: (i) tackling the MNCP defined by (16)-(19) via (MNCPOpt); (ii) considering the LCP originated by the pyramidal approximation to the Coulomb cone formulated by (20) via (LCPOpt).

4.2.1 MNCP

With two rolling contacts, problem (MNCPOpt) has 16 variables. Matrices $\tilde{\boldsymbol{A}}_1 \in \mathbb{R}^{2\times 6}$ and $\tilde{\boldsymbol{A}}_2 \in \mathbb{R}^{4\times 6}$, from equations (16) and (19), respectively, were computed in MATLAB, using the Robotics TOOLBOX [4]. Vector $\boldsymbol{b}_{\mathcal{R}} \in \mathbb{R}^6$ was randomly generated in $[-5,5]^6$. Out of the two hundred tests, 183 were successfully solved (92%). The results are visually displayed in Figure 4, a bar chart of $\lfloor -\log_{10}|f_M^*|\rfloor$ *versus* number of tests. The high frequency of tests with $\lfloor -\log_{10}|f_M^*|\rfloor = 10$ is perhaps related with the chosen value for the tolerance used as stopping criterion.

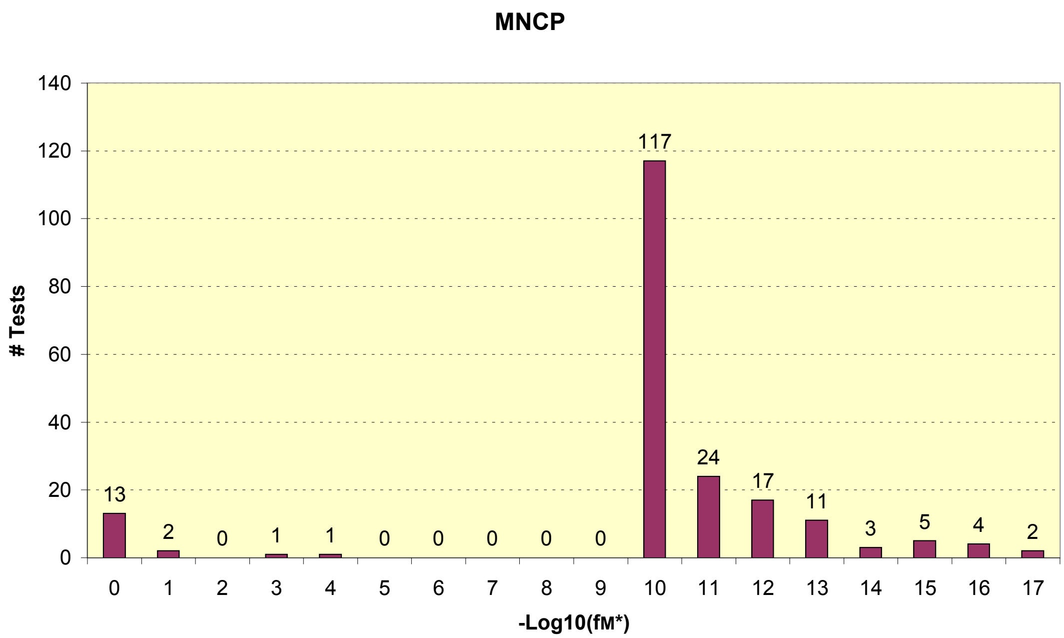

Figure 4: Objective function value distribution of (MNCPOpt)

4.2.2 LCP

The problem (LCPOpt) associated with two rolling contact points has 20 variables and its matrix $Q \in \mathbb{R}^{10\times 10}$ was generated in MATLAB by means of the Robotics TOOLBOX [4]. Since vector $\boldsymbol{d} \in \mathbb{R}^{10}$ is such that $d^T = (\boldsymbol{b}_{\mathcal{R}}^T, 0, 0, 0, 0)$, to ensure that we were solving the relaxed versions of the instances considered in the previous subsection, vector $\boldsymbol{b}_{\mathcal{R}} \in \mathbb{R}^6$ was randomly generated in $[-5,5]^6$ with the same seeds as before. The number of problems successfully solved was 194, in a total of 200 (97%). As before, the class characterized by $\lfloor -\log_{10}|f_L^*|\rfloor = 10$ is associated with the highest frequency of outcomes. Also notice that it plays the role of a threshold, marking the beginning of magnitude values for the objective function that are associated with significant number of tests. Figure 5 contains the bar chart of $\lfloor -\log_{10}|f_L^*| \rfloor$ *versus* number of tests.

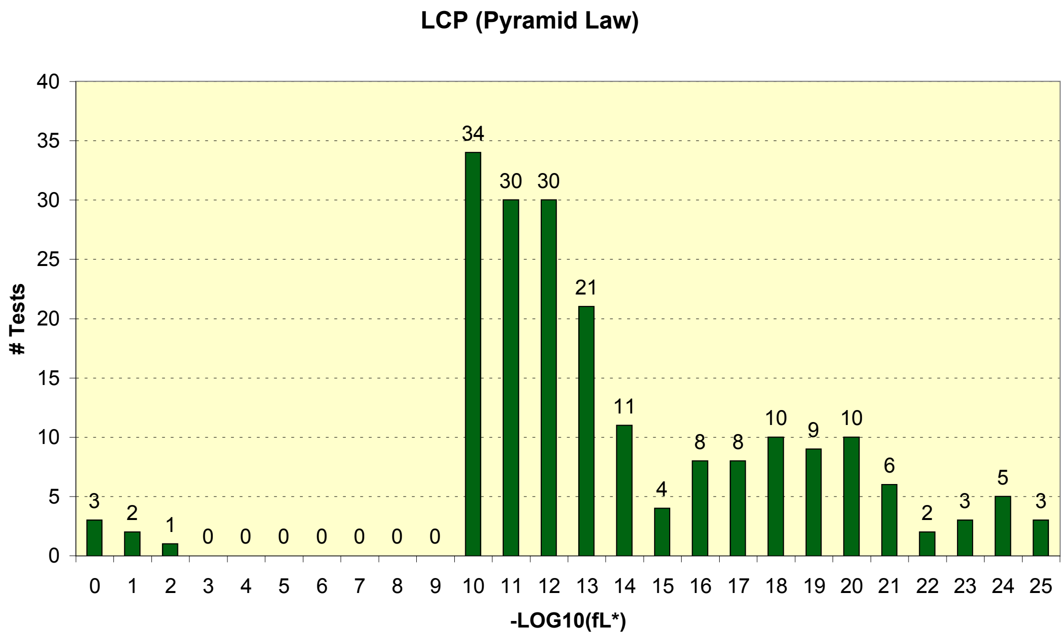

Figure 5: Objective function value distribution of (LCPOpt)

4.2.3 MNCP $\times$ LCP

Comparing the two approaches for solving the all rolling case with two contact points, Tables 1 and 2 summarize the average computational results. In terms of computational efforts, figures of Tables 1 and 2 pointed to the MNCP being around nine times more demanding than the LCP.

Table 1: CPU time in seconds

	(MNCPOpt)	(LCPOpt)
minimum	0.000	0.000
average	0.200	0.030
maximum	8.740	0.170

With respect to the quality of the solution obtained in each case, a further analysis of the results is necessary. One desired feature of the solution of a problem with rolling contacts is to encompass a possible transition from rolling to sliding in a coherent fashion, that is, ensuring that the tangential accelerations oppose the tangential contact forces. The Coulomb friction cone defined by (9) together with equation (12) guarantee such conditions for the MNCP. The approximate model of the pyramid law, given by (14)-(15), however,

Table 2: Average results of code easy

	Outer iterations	Functional evaluations	Inner iterations	Matrix-vector products
(MNCPOpt)	57.3	76.3	984.2	1150.8
(LCPOpt)	7.5	8.9	90.8	126.3

does not enforce that (a_{jt}, a_{jo}) directly oppose (c_{jt}, c_{jo}), for $j \in \mathcal{R}$. The colinearity of the tangential acceleration and force was tested at each contact point for the successfully solved problems. Considering the MNCP approach, colinearity was obtained in 122 and 128 tests, for contact points 1 (cp_1, $122/183 = 67\%$) and 2 (cp_2, $128/183 = 70\%$), respectively. For the pyramid model, the opposition holds in 97 and 153 tests, for contact points cp_1 and cp_2, respectively. Analysing in details the failures, one can observe that outcomes with the contact force at the corner of the pyramid were not so frequent as claimed in [16]. Figure 6 provides a scheme of the various reached possibilities, summarizing the frequency of results in each case.

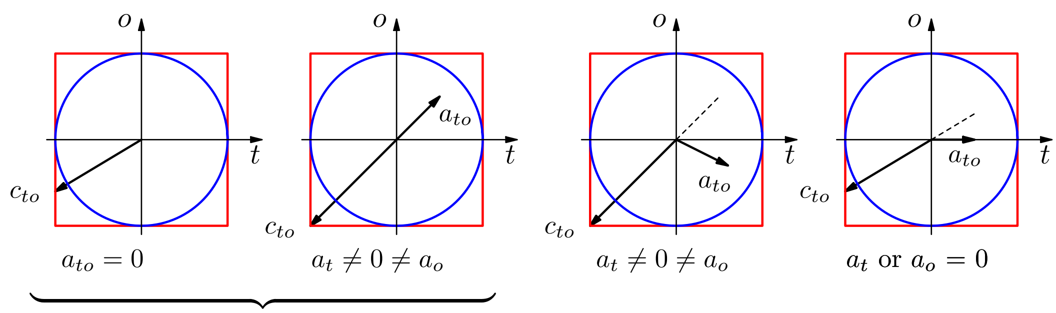

cp_1	97/194 (50%)	26/194 (13%)	71/194 (37%)
cp_2	153/194 (79%)	11/194 (6%)	30/194 (15%)

Figure 6: Relationship between tangential forces and accelerations

Another observation concerning the quality of results is the following: the pyramid contains the Coulomb cone, but with the pyramid law the contact forces might lay outside the Coulomb cone. In fact, this was the case for several problems: 106 out of 200 for cp_1 (53%) and 53 out of 200 for cp_2 (27%).

Comparing the transitions, from rolling to rolling, sliding or breaking contacts, the agreement between both aproaches ocurred as follows: out of the 178 simultaneously successfully solved tests, 98% in cp_1 and 96% in cp_2 pointed to the same transition.

Ideally one would test the practical validity of the sufficient conditions of Theorem 1 by building a test set of problems with known solutions. In this case it is straightforward to decide whether the solution obtained is the real solution or a spurious one. Taking into consideration the fact that, in our setup, part of the data was randomly generated, we had no previous knowledge of the solution or in fact that the problem admitted one. This poses an added difficulty regarding the appraisal of the solutions obtained, for even though a “solution” to a given problem may be stationary from a numerical point of view, it is sometimes far from a true stationary point. In our case, we elected the colinearity test as a indicator of the solutions' physical meaning. We selected the successfully solved tests of the MNCP formulation that failed the colinearity test in either of the two contacts, a total of 79. Of these, 78 exhibited singular $\boldsymbol{g_v}$ at the final solution. This means the Schur complement didn't exist at these points and the conditions of Theorem 1 did not hold. The unique remaining problem satisfied both conditions (the Schur complement was a row sufficient S matrix), had objective function value 4×10^{-11} and norm of the projected gradient equal to 4×10^{-6}. Thus the point obtained is numerically but not truly stationary.

5 Final remarks

This work shows that it is worthwhile using ready-made, available software for bound-constrained optimization to solve the complementarity problems stemming from dynamic multi-rigid-body models. In particular, this approach allowed the direct handling of the three-dimensional multi-rigid-body model based on the Coulomb friction law, instead of its approximation, as done in [16]. We also point out that the merit function does not involve penalization parameters or multipliers. Finally, the merit function is as well behaved as the original functions, it does not introduce troublesome characteristics.

Although the problems solved are still small-scale ones, the preliminary numerical experiments indicate that the approach is promising for solving the model with friction.

References

[1] R. Andreani, J. M. Martínez, *On the solution of bounded and unbounded mixed complementarity problems*, Optimization, 50 (2001), 265–278.

[2] R. Andreani, J. M. Martínez, *Solving complementarity problems by means of a new smooth contrained nonlinear solver*, in M. Fukushima and L. Qi, eds., *Reformulation: Nonsmooth, Piecewise Smooth, Semismooth and Smoothing Methods*, Kluwer, Netherlands (1999), pp. 1–24.

[3] F. Buffo, A. Friedlander, M. C. Maciel, *Dynamic multi-rigid body contact problems and linear complementarity technics*, 22nd Iberian Latin-American Congress on Computational Methods in Engineering/2nd Brazilian Congress on Computational Mechanics - XXII CILAMCE 2001, Campinas, SP, Brazil (2001), CD-Rom.

[4] P. I. Corke, *Robotics TOOLBOX for MATLAB* (Release 7), April 2002, available at `http://www.cat.csiro.au/cmst/staff/pic/robot`.

[5] M. C. Ferris, C. Kanzow, T. S. Munson, *Feasible descent algorithms for mixed complementarity problems*, Math. Prog. Tech. Rep. 1998-04, Computer Science Department, University of Wisconsin, Madison, Wisconsin (1998).

[6] M. C. Ferris, J.-S. Pang, *Engineering and economic applications of complementarity problems*, SIAM Rev., 39 (1997), 669–713.

[7] M. Fiedler, V. Pták, *Some generalizations of positive definiteness and monotonicity*, Numer. Math., 9, (1966), 163–172.

[8] A. Friedlander, J. M. Martínez, S. A. Santos, *A new trust region algorithm for bound constrained minimization*, Appl. Math. Optim., 30 (1994), 235–266.

[9] A. Friedlander, J. M. Martínez, S. A. Santos, *Solution of linear complementarity problems using minimization with simple bounds*, J. Global Optim., 6 (1995), 253–267.

[10] P. T. Harker, J.-S. Pang, *Finite-dimensional variational inequality and nonlinear complementarity problems: a survey of theory, algorithms and applications*, Math. Prog., 48 (1990), 161–220.

[11] J. J. Júdice, *Algorithms for linear complementarity problems*, in E. Spedicato, ed., *Algorithms for Continuous Optimization*, Kluwer, Netherlands (1994), 435–474.

[12] N. Krejić, J. M. Martínez, M. P. Mello, E. A. Pilotta, *Validation of an Augmented Lagrangian algorithm with a Gauss-Newton Hessian approximation using a set of hard-spheres problems*, Comput. Optim. Appl., 16 (2000), 247–263.

[13] R. M. Murray, Z. Li, S. S. Sastry, *A Mathematical Introduction to Robotic Manipulation*, CRC Press, Florida (1994).

[14] J.-S. Pang, *Complementarity problems*, in R. Horst, P. Pardalos, eds., *Handbook in Global Optimization*, Kluwer, Netherlands (1994), pp. 271–338.

[15] J.-S. Pang, J. C. Trinkle, *Complementarity formulations and existence of solutions of multi-rigid-body contact problems with Coulomb friction*, Math. Program., 73 (1996), 199–226.

[16] J. C. Trinkle, J.-S. Pang, S. Sudarsky, G. Lo, *On dynamic multi-rigid-body contact problems with Coulomb friction*, Technical report 95-003, Department of Computer Sciences, Texas A&M University, College Station (1995), 47 p.

[17] J. C. Trinkle, J.-S. Pang, S. Sudarsky, G. Lo, *On dynamic multi-rigid-body contact problems with Coulomb friction*, Z. Angew. Math. Mech., 77 (1997), 267–279.

[18] J. A. Tzitzouris, Jr., *Numerical Resolution of Frictional Multi-Rigid-Body Systems via Fully Implicit Time-Stepping and Nonlinear Complementarity*, Ph.D. Thesis, Department of Mathematical Sciences, The Johns Hopkins University, Baltimore, MD (2001), 154 p.